Air Quality, Atmosphere & Health (2018) 11:1021–1035
https://doi.org/10.1007/s11869-018-0602-4

Impact of biogenic emissions on early summer ozone and fine particulate matter exposure in the Seoul Metropolitan Area of Korea

Hyeon-Kook Kim[1] · Chang-Keun Song[1] · Kyung Man Han[2] · Yang Dam Eo[3] · Chul Han Song[2] · Rokjin Park[4] · Sung-Chul Hong[5] · Sang-Kyun Kim[5] · Jung-Hun Woo[3]

Received: 27 October 2017 / Accepted: 3 July 2018 / Published online: 11 July 2018

Abstract

Understanding how ozone (O_3) and fine particulate matter (PM) formation respond to the precursor concentrations in the presence of biogenic emissions (BEs) and thereby changes in health effects can be a key step to design effective air quality management plans. This is particularly true in the Seoul Metropolitan Area (SMA), where future significant controls of anthropogenic sources of O_3 and $PM_{2.5}$ precursors are expected. In this paper, we investigate the effects of BEs on O_3 and fine PM ($PM_{2.5}$) concentrations during a strong photochemical air pollution season in the SMA in Korea. O_3 and $PM_{2.5}$ levels are modeled with and without BEs in June 2008. Further, we perform the health impact assessments (HIA) of O_3 and $PM_{2.5}$ concentration changes due to BEs to seek useful implications for air quality management by utilizing the adjusted exposure concentration fields for O_3 and $PM_{2.5}$ with an observation fusing (OBF) method. With BEs, daily maximum 8-h average O_3 (maximum 8-h O_3) and secondary organic aerosol (SOA) concentrations in the SMA increase by 17 and 474%, respectively. These increments are associated with significant consumption of photochemical oxidants (O_x), such as a ~60% reduction in $OH^{\cdot}$ radicals. The reduction in O_x, conversely, lowers the production of secondary inorganic aerosols (SIOAs) by 2.7%. Adjusted O_3 and $PM_{2.5}$ exposure metrics and the subsequent HIA reveal that large mean increments of O_3, about 8.43 ppb, due to BEs are responsible for approximately 62 all-cause premature mortalities in the SMA in June. However, mean increment of $PM_{2.5}$ due to BEs is approximately 0.3 μg m^{-3} and results in negligible impacts on the all-cause mortality. Significant correlations of O_3 and mortality rates (MR) with the VOC/NO_x ratios across the SMA suggest that controlling volatile organic compounds (VOCs) from anthropogenic sources can be a priority to reduce O_3 levels and population health risks in the SMA. Specifically, linear relationships of log [O_3] and log [MR] to log [VOC/NO_x] ensure that a 10% decrease in the VOC/NO_x ratios through the VOC abatements would lead to a 1.5% decrease in the O_3 levels and a 4.3% decrease in the MR on average across the SMA.

Keywords Health impact assessment · Ozone · Particulate matter · Biogenic emissions · Air quality modeling

Introduction

Urban air pollution can affect human mortality and morbidity. The major causes of such adverse effects are exposure to ozone (O_3) and particulate matter (PM) with a diameter of up to 2.5 μm (hereafter, $PM_{2.5}$) (WHO 2013). Populations in most East Asian metropolitan city areas have been exposed to hazardous levels of O_3 and PM air pollution, increasing the risk of premature death. For example, a 10 μg m^{-3} increase in maximum 8-h average O_3 (maximum 8-h O_3) concentration in summer was associated with a 0.45% (95% posterior interval (PI) 0.36–0.55) increase in daily mortality in Korea (Chen et al. 2014a). A 10 μg m^{-3} increase in 24-h average $PM_{2.5}$ (mean 24-h $PM_{2.5}$) was associated with a 0.36% (95% CI 0.16–1.73) increase in daily mortality in Shanghai metropolitan area in China (Kan et al. 2007).

Electronic supplementary material The online version of this article (https://doi.org/10.1007/s11869-018-0602-4) contains supplementary material, which is available to authorized users.

✉ Jung-Hun Woo
jwoo@konkuk.ac.kr

[1] School of Urban and Environmental Engineering, Ulsan National Institute of Science and Technology, Ulsan 44919, South Korea

[2] School of Environmental Science and Engineering, Gwangju Institute of Science and Technology, Gwangju 61005, South Korea

[3] Division of Interdisciplinary Studies, Konkuk University, Seoul 05029, South Korea

[4] School of Earth and Environmental Science, Seoul National University, Seoul 08826, South Korea

[5] Climate and Air Quality Research Department, National Institute of Environmental Research, Incheon 22689, South Korea

Reducing the risks of population exposure to O_3 and $PM_{2.5}$ has been a focus of air quality control policy due to heightened awareness and concern over the adverse health effects of these pollutants (Wesson et al. 2010; Hubbell 2012). In this context, the Korean Ministry of Environment (MoE) included O_3 and $PM_{2.5}$ as priority control targets in the second phase of the Seoul Metropolitan Air Quality Improvement Plan (SMAQIP-II) for 2015–2024 (MoE 2015). The SMAQIP-II highlights the need to establish a risk-based management strategy, including reducing population health risks in areas experiencing high concentrations of O_3 and $PM_{2.5}$, namely, hotspots, in the Seoul Metropolitan Area (SMA) (MoE 2015). This risk-based approach requires consolidated scientific data based on an improved understanding of the roles and effects of various emissions on air quality, population exposure, and health risk (Hubbell 2012). However, there is limited number of studies integrating such multiple aspects and providing useful insights for future design of a risk-based air quality management in Korea.

Formation of O_3 and secondary organic aerosols (SOAs) involves complex photochemical processes that are sensitive to the emission strength of precursor species, such as volatile organic compounds (VOCs) and NO_x (Atkinson 2000; Finlayson-Pitts and Pitts 2000). In particular, biogenic emissions (BEs), which generally contain highly reactive VOC species, can significantly contribute to O_3 and SOA formation in urban and surrounding regional atmospheric environments with high NO_x emissions from anthropogenic sources and prevailing strong sunlight (Atkinson and Arey 2003). Recent 3-D photochemical transport modeling experiments in East Asia show the significant contribution of BEs to O_3 and SOA production through the interactions with anthropogenic emissions in urban metropolitan areas. For example, at the Taehwa Research Forest site in the SMA of Korea in June 2011, increases of 5–20 ppb in daytime hourly O_3 were simulated due to the effect of BEs (Kim et al. 2013). In addition, across 191 sites within the Tokyo Metropolitan Area (TMA) of Japan in August 2005, an average increase of 14 ppb was simulated in the daytime maximum O_3, and dominant fractions of SOAs from BEs were simulated in the organic aerosol composition (Chatani et al. 2015).

Previous studies have suggested two important factors in emission behavior. First, from an air quality perspective, the impact of BEs on urban O_3 and PM pollution can vary by region due to different emission strengths and photochemical regimes. Second, from a health risk perspective, certain changes in O_3 and PM air quality due to BEs can change the level of population exposure. These two factors are connected, but few studies have investigated them simultaneously. A more thorough study of these interconnected factors could provide useful information for risk-based air quality management to agencies concerned with air quality and human health protection.

In this study, we first examined BE-related changes in O_3 and $PM_{2.5}$ concentrations using a 3-D air quality model (AQM) and subsequently assessed the health impacts due to these concentration changes. In the health impact assessment (HIA) applying AQM, reducing biases in predicted concentration fields is an important task (Huang et al. 2017; Dionisio et al. 2016; Chen et al. 2014b). Thus, we applied an observation data fusing (OBF) approach combining the observations and modeled data with a spatial interpolation method to produce more improved air pollution concentration fields for HIA. As the study region, we choose the SMA in Korea. The SMA is a highly developed urban community, where various anthropogenic emission sources and densely vegetated areas coexist.

Method and data

Modeling framework

The implemented air quality simulation framework includes four modeling systems. The first system is the Fifth-Generation NCAR/Pennsylvania State Meso-scale Model (MM5) for meteorology (Grell et al. 1994), assimilated with 10 m Advanced Scatterometer (ASCAT) wind data (Park et al. 2011). We further adjusted the MM5 outputs using monitored temperature, wind speed, and rain intensity data from 11 sites (see Fig. 1b) maintained by the Korea Meteorological Administration. The modeled temperature, wind speed, and rain intensity values were adjusted at every grid cell by using a set of temporally varying observation-to-model ratios for corresponding variables (Kim et al. 2014). The resultant temperature, wind speed, and rain data show reduced bias uncertainties and almost perfectly capture the observations (Fig. S1). The second system is the Sparse Matrix Operator Kernel Emissions (SMOKE) model for anthropogenic emissions, updated with detailed spatial and temporal surrogate databases in Asia (Woo et al. 2012). The third system is the Model of Emissions of Gases and Aerosols from Nature (MEGAN) v2.04 (Guenther et al. 2006) for BEs, updated with the Korean plant functional type (KORPFT) information (Kim et al. 2014). The last system is the Community Multiscale Air Quality (CMAQ) v4.6 for modeling chemistry and transport (Byun and Schere 2006). We used the State Air Pollution Research Center mechanism version 1999 (SAPRC-99) (Carter 2000) for the CMAQ gas-phase chemical mechanism. We also used the AERO3 module (Binkowski and Roselle 2003), which includes the SOA_NEWT module (Schell et al. 2001) for SOA formation and the ISORROPIA module (Nenes et al. 1998) for inorganic aerosol equilibrium, for CMAQ aerosol formation.

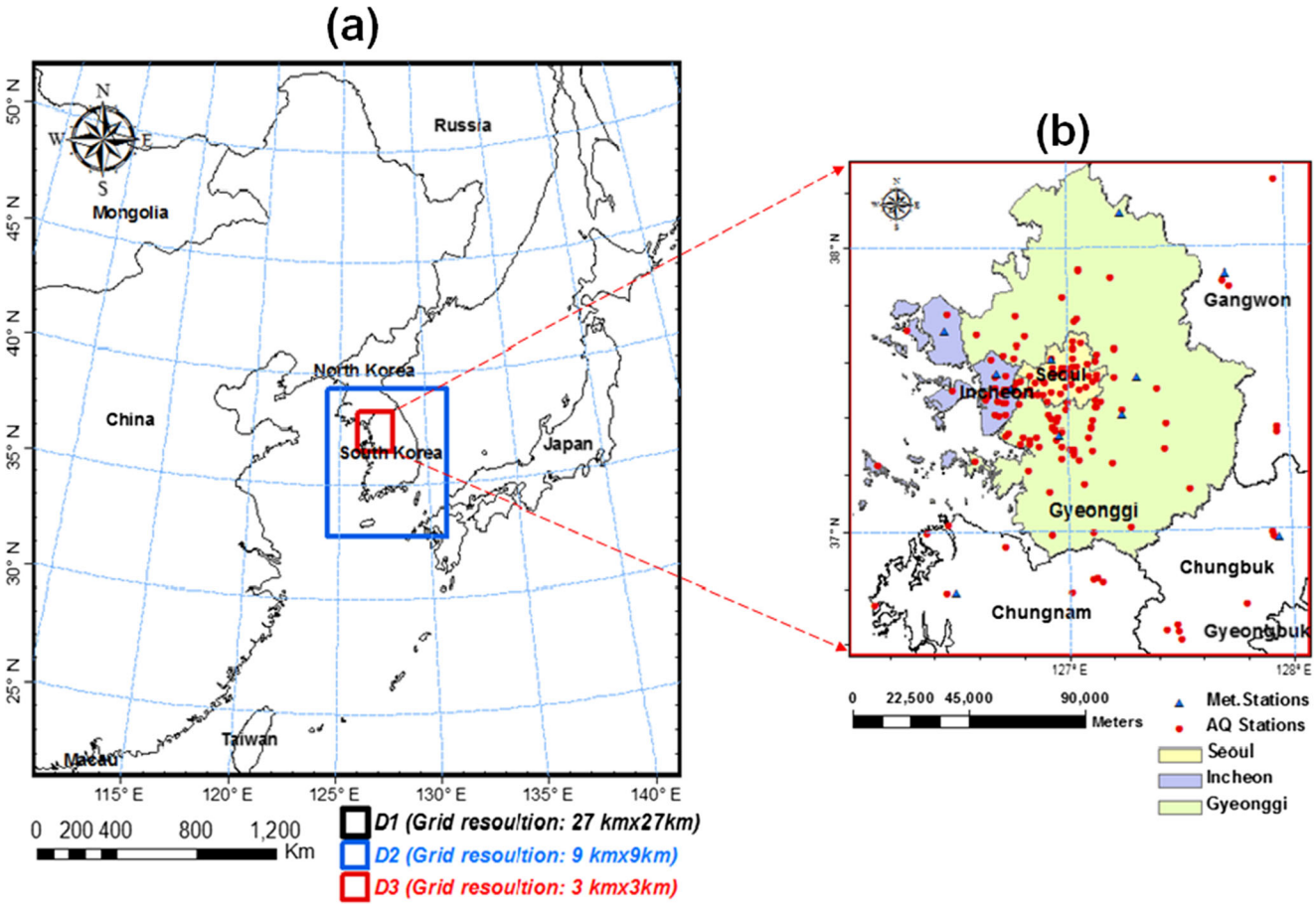

Fig. 1 The modeling domain. The smallest domain is a 3 × 3 km^2 grid system domain covering our study area, the SMA, Seoul, Incheon, and Gyeonggi. *Met.*, meteorological; *AQ*, air quality

Air quality simulation

We used a three-domain system for meteorology and air quality simulation, consisting of 20 vertical layers to resolve the atmosphere between the surface and 100 hPa in the sigma vertical coordinate. The three domains include horizontal resolutions of 27 × 27 km^2 for the largest, 9 × 9 km^2 for the second largest, and 3 × 3 km^2 for the smallest domain, for the nested simulations (refer to Fig. 1a). The anthropogenic emission inventory used for SMOKE emission processing is a merged version of the INTEX 2006 (Zhang et al. 2009) and TRACE-P 2000 inventories (Streets et al. 2003). More details on the simulation are documented in Kim et al. (2014). Based on these emissions and meteorological inputs, we performed one-way-nested CMAQ simulations at the three domains for May 28–June 30, 2008, with a 4-day spin-up period. We used June as our study period because it lies within a major photochemical pollution season in Korea. Detailed analyses of the change in O_3 and $PM_{2.5}$ due to the presence of BEs were performed focusing on the smallest domain, including the SMA region with the highest resolution modeling grids (Fig. 1b).

Performance evaluation

To examine the BE-driven O_3 and $PM_{2.5}$ pollution changes, we first performed CMAQ simulations assuming the presence of BEs ([A + B] scenario) and their absence ([A] scenario). Second, we developed air pollution metric sets using simulated air quality fields for O_3 and $PM_{2.5}$ with a 3 km × 3 km resolution for each scenario. The chosen pollution metrics include daily maximum 8-h O_3, maximum 1-h O_3, mean of 8-h average O_3 (mean 8-h O_3), mean 24-h PM_{10}, and mean 24-h $PM_{2.5}$. Third, we compared the O_3 and PM metrics derived from the simulated concentration fields with corresponding measurements in the ambient air quality monitoring network, 148 ambient stations for O_3 and for PM (Fig. 1b). The aim of this comparison was to investigate the effect of added BEs on the modeling performance for the pollution metrics. Meanwhile, it should be noted that for PM, we only checked the mean 24-h PM_{10} performance because $PM_{2.5}$ observations were unavailable. For performance criteria, we referred to Russell and Dennis (2000) for O_3 and Boylan and Russell (2006) for PM_{10}.

Observation data-fusion

To obtain less-biased O_3 and $PM_{2.5}$ concentration fields for HIA, we conducted the observation data-fusion (OBF) based on the inverse distance weighting (IDW) technique using the differences between observations and CMAQ predictions at the locations of surface monitoring sites (Chen et al. 2014b). The IDW was conducted in the R statistical computing environment (R Core Team 2018) using the gstat package (Pebesma and Graeler 2018). The observation data-fused CMAQ (CMAQ-OBF) concentration fields were derived by the following three steps:

Step (1) Primarily for the [A + B] case, the location-specific differences between observations and CMAQ predictions (δc_i) for O_3 and PM_{10} are interpolated to all grid cells applying the following IDW method:

$$\delta \mathrm{c}(x) = \sum_{i=1}^{N} \frac{w_i(\mathrm{x})\delta c_i}{\sum_{j=1}^{N} w_i(x)} \quad (1)$$

$$w_i(x) = d(x, x_i)^{-p} \quad (2)$$

where x is the center of a grid cell in the model domain, $w_i(x)$ is the weight represented by the inverse of the distance between the interpolation location x and the observation sites x_i raised to the power (p), and $\delta c(x)$ is the estimated difference between the expected pollutant concentration and the model prediction at the grid cell.

Step (2) The expected (i.e., observation fused) concentration ($c_p^{'}(x)$) for O_3 and PM_{10} for the [A + B] case is derived at each grid cell by the following:

$$c_p^{'}(x) = c_p(x) + \delta c(x) \quad (3)$$

Step (3) O_3 and $PM_{2.5}$ concentration fields for the [A] case are corrected by using the output from step 2 (i.e., $c_p^{'}(x)$). For O_3, the concentrations for the [A] case are directly obtained by multiplying the $c_p^{'}(x)$ values for O_3 by the CMAQ simulated [A]-to-[A + B] ratios for O_3. Meanwhile, derivation of $PM_{2.5}$ concentrations for the [A] case requires one more procedure. Firstly, PM_{10} fields for the [A] case are derived by multiplying the $c_p^{'}(x)$ values of PM_{10} by the corresponding CMAQ [A]-to-[A + B] ratios. Then, the $PM_{2.5}$ fields for the [A] case are corrected by multiplying the previously derived PM_{10} fields for the [A] case by the CMAQ $PM_{2.5}$-to-PM_{10} ratios.

Health impact assessment

We calculated the mortalities (M) that are attributable to the BE-driven O_3 and $PM_{2.5}$ pollution changes by using the following equation:

$$M = (1-\exp(-\beta \Delta C))M_0 P \quad (4)$$

where β is the health impaction function (HIF) parameter and ΔC is the daily O_3 and $PM_{2.5}$ pollution changes (i.e., ΔO_3 and $\Delta PM_{2.5}$) for June 2008. M_0 is the baseline mortality incidence rate for June 2008 and P is the total population from 0 to 99 years old. To derive ΔO_3 and $\Delta PM_{2.5}$, we used the CMAQ-OBF concentration fields with two scenarios (i.e., [A + B] and [A]). By taking the difference of these two sets of concentration fields, we developed daily ΔC for O_3 and $PM_{2.5}$ at each 3 km × 3 km model grid unit.

The population (P) was based on the 2010 Korea population census data from the Statistics Korea (KOSTAT: http://kostat.go.kr/). We mapped these census data into the finer administrative level (Si-Gun-Gu) grid-shape files using an ArcGIS tool. Then, we distributed the mapped data into each of the model grid cell by zonal averaging and area weighting methods under the assumption of evenly distributed population within a base geographic unit. The constructed population distribution well illustrates that Seoul is the most populated region (Fig. S2, a). The used death count data were constructed based on the daily death counts at the Si-Gun-Gu unit for June 2008 obtained from KOSTAT. In our short-term HIA, we only considered mortalities due to all causes (all-cause). The all-cause excludes the mortalities by accidental cases. According to the International Classification of Disease, Tenth Revision (ICD-10; WHO 1994), we extracted the death counts for all causes (codes A00–R99). Like population, we constructed the death count distribution datasets for all-cause at the 3 km × 3 km resolution. Using the pre-constructed population and death count distribution data sets, we created the baseline mortality incidence rates at 3 km × 3 km resolution during June 2008. The constructed map for the incidence rate indicates that Seoul is the most vulnerable region to the all cause (Fig. S2, b).

For the HIF parameter (β), we chose the excess risk (ER) values drawn by Chen et al. (2014a) and Lee et al. (2015) for O_3 daily mortality across seven Korean cities during summer and for $PM_{2.5}$ short-term mortality across 11 East Asian cities (including two metropolitan cities in Korea) during warm season, respectively (Table 1). We converted the chosen ERs into β values by using the following relationship:

$$\beta = ln(RR)/\Delta C \quad (5)$$

Table 1 Main characteristics of the excess ratio (ER (%)) at all ages adopted for this study. The tabulated ERs are associated with a change in O_3 and $PM_{2.5}$ concentrations of 10 ppb and 10 μg m^{-3}, respectively

Metric	Study area	Period	Mean concentration	ER (%)	95% CI	Reference
Max 8-h O_3	7 Korean cities	1999–2010 summer	44.1–50.3	0.89	(0.71, 1.09)	Chen et al. (2014a)
Mean 24-h $PM_{2.5}$	11 East Asian cities including two Korean cities (Seoul and Busan)	2001–2009 warm season (April–September)	17.7–69.9	0.29	(− 0.05, 0.62)	Lee et al. (2015)

where *RR* is the relative risk of mortality (RR=(1 + *ER*(%))/100) for a given Δ*C* for a pollutant. More details about the derivation of health impact functions are well-documented at the US EPA (2012).

Results and discussions

Changes in emissions

The emissions from the two scenarios are summarized in Table 2 for major particulate and gaseous species. The biogenic source causes a significant increase in total non-methane VOC (NMVOC) emissions, although the number for Seoul is low. The predicted increases in total NMVOC emissions were 132% for the entire domain, 56% in the SMA, 2% in Seoul, 19% in Incheon, and 119% in Gyeonggi, and 434% in the other regions.

Meanwhile, the contribution of the biogenic NO to total NO_x (= NO + NO_2) emissions in the domain was small, showing an increase of less than 2% compared to the total (0.7% in the entire domain, 0.3% in the SMA, 0.01% in Seoul, 0.1% in Incheon, and 0.6% in Gyeonggi, and 2% in the other regions). Although the relative amount of biogenic NO was small, its role in the O_3 and secondary aerosol related photochemistry was noteworthy in the SMA. The "Effects on O_3 and $PM_{2.5}$ concentrations" section gives a detailed explanation of this topic. Meanwhile, it should be noted that our emission modeling considers anthropogenic emissions as the only sources of NO_2, SO_2, NH_3, and $PM_{2.5}$. Thus, these species show no changes in emissions between scenarios.

The spatial distribution plots reveal that Seoul is a hotspot region for anthropogenic emissions of $PM_{2.5}$, NO_x, NH_3, SO_2, and NMVOCs (Fig. 2a–d and Fig. 3a). Seoul has no prevailing significant BE sources (Fig. 3b,e), but it is surrounded by abundant BE sources for NMVOC and NO. In the [A] scenario, relatively low values of VOC/NO_x emission ratios (unit mol C mol^{-1}) were distributed across the domain (i.e., VOC/NO_x < 4). However, in the [A + B] scenario, there were noticeable increases in the VOC/NO_x emission ratios, exceeding 500 in some suburban and rural areas of Gyeonggi, Incheon, and their neighboring locations. The VOC/NO_x emission ratios were not significantly altered in Seoul (Fig. 3g–i).

Evaluation of air quality metrics before and after OBF

The performance statistics based on raw CMAQ results for individual O_3 and PM_{10} metrics are summarized in Table S1. The inclusion of BEs readily improved the model performance for O_3 and PM. Nonetheless, future efforts should achieve better predictions. The differences in monthly averaged air quality metrics between the [A] and [A + B] scenarios were not small, especially for O_3, which showed an overall difference of 5–7 ppb. For maximum 1-h O_3, the normalized mean bias (NMB) and the normalized mean error (NME) of the CMAQ-[A + B] case exceeded the US EPA's model performance standards (MPS) of ≤ 15% for NMB and ≤ 35% for NME, by 4 and 1%, respectively. For maximum 8-h O_3, the NMB for the CMAQ-[A + B] case exceeded the US EPA's MPS by 6%, whereas the NME fell within the standards. For mean 24-h PM_{10}, the mean fractional bias (MFB) was satisfactory for the MPS (i.e., MFB ≤ ± 30%) but the mean fractional error (MFE) exceeded the MPS (i.e., MFE ≤ + 75%) by 13%. The correlations between all metric variable data for O_3 and PM_{10} derived from the raw CMAQ results and corresponding metric data from monitoring stations were moderate (r = 0.42–0.64). Overall, the raw CMAQ-[A + B] results show large under-predictions when compared to the observations.

Because the accuracy of the air quality concentration fields is an important factor for the reliable health impact assessment (Huang et al. 2017; Dionisio et al. 2016; Chen et al. 2014b), we conducted the bias correction for the raw CMAQ-[A + B] results by applying the OBF method described in the "Observation data-fusion" section. To evaluate the OBF method, we performed cross-validation (CV) at randomly selected (RS) 16 monitors (10% of total number of monitors). For CV, we first performed the OBF at all grid cells in the model domain after withholding the data at the locations of the RS 16 monitors. After that, we evaluated the OBF results (i.e., CMAQ-OBF for the [A + B] case) at the locations of the RS 16 monitors. Figure S3 and Table S2 indicate the significant improvements after OBF in reproducing the time changes and the reductions of bias and errors in metric values for O_3 and PM_{10} at the RS 16 sites compared to the raw CMAQ results. This implied that OBF using all 148 monitors' data can further improve the accuracy of O_3 and PM_{10} air quality metrics. In

Table 2 Summary of the emissions during June 2008 used in the simulations (unit gigagram month^{-1}). The SMA region includes Seoul, Incheon, and Gyeonggi. "[A + B]" and "[A]" indicate the combined anthropogenic-biogenic case and anthropogenic-only case, respectively

		Source	NO	NO_2	NMVOC	NH_3	SO_2	$PM_{2.5}$
Domain all		[A]	19.754	1.76	18.32	4.29	9.39	6.92
		[A + B]	19.897	1.76	42.52	4.29	9.39	6.92
SMA	Seoul	[A]	6.042	0.54	6.36	0.57	2.92	1.81
		[A + B]	6.043	0.54	6.51	0.57	2.92	1.81
	Incheon	[A]	1.850	0.16	1.82	0.25	0.68	0.46
		[A + B]	1.853	0.16	2.17	0.25	0.68	0.46
	Gyeonggi	[A]	6.349	0.57	6.44	1.6	3.75	2.93
		[A + B]	6.392	0.57	14.12	1.6	3.75	2.93
	SMA-Total	[A]	14.241	1.27	14.62	2.41	7.35	5.2
		[A + B]	14.287	1.27	22.79	2.41	7.35	5.2
Other regions		[A]	5.513	0.49	3.69	1.88	2.04	1.72
		[A + B]	5.610	0.49	19.72	1.88	2.04	1.72

reality, the OBF with full monitoring dataset led to great improvements in reproducing the temporal variability (Fig. 4) and large reductions of prediction bias and errors (see Tables 3 and S1) for O_3 and PM_{10} air quality metric values compared to the raw CMAQ results. For example, the OBF using full monitor's data led to the increased R^2 values from 0.25 to 0.71 for maximum 8-h O_3 and from 0.19 to 0.85 for 24-h mean PM_{10}. The size of bias also reduced from 9.5 to 0.27 ppb for maximum 8-h O_3 and 5.0 to 0.64 μg m^{-3} for 24-h mean PM_{10}. Furthermore, the reconstructed O_3 and PM_{10} air

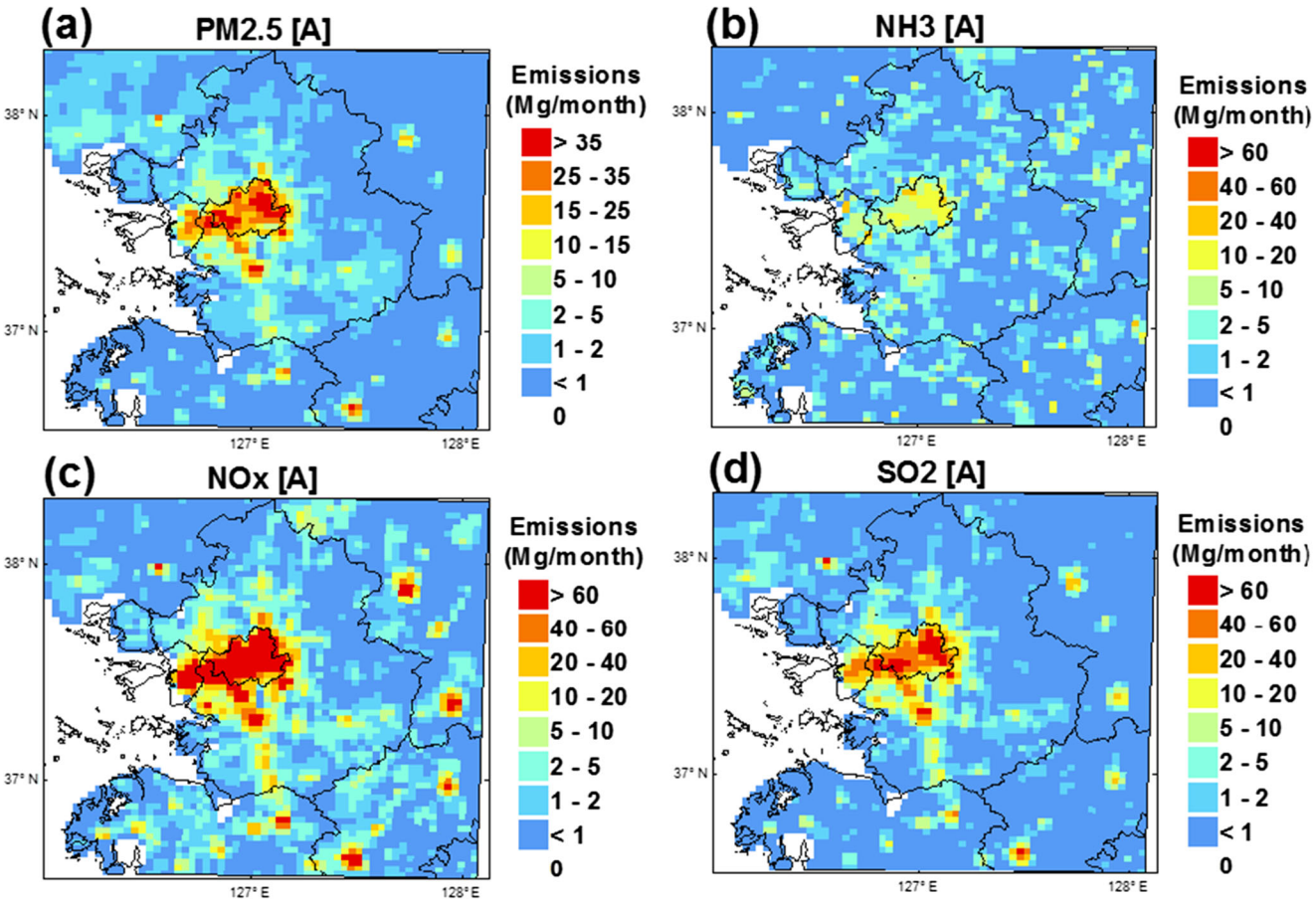

Fig. 2 Distributions of monthly anthropogenic aerosol and gaseous emissions in the study domain. "[A]" indicates the anthropogenic-only case

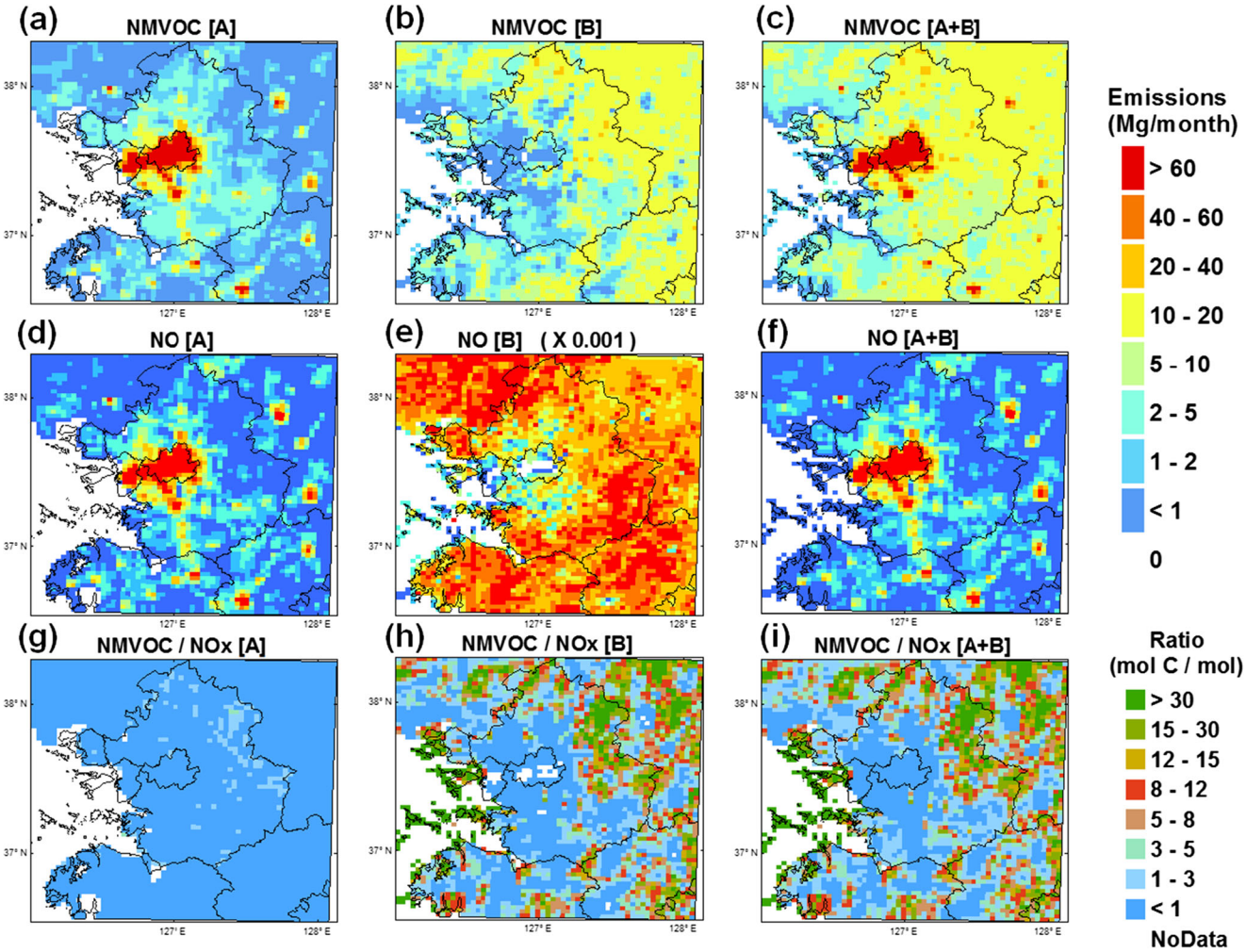

Fig. 3 Emission distributions of important precursor species for O_3 and aerosol formation and the VOC/NO_x ratio. "[A + B]" indicates the combined anthropogenic-biogenic case

quality metric fields for the [A] case through the step 3 in the "Observation data-fusion" section also obtained substantial improvements in the performance while sustaining their relative magnitude to the corresponding data for the [A + B] case (i.e., [A]-to-[A + B] ratio).

Effects on O_3 and $PM_{2.5}$ concentrations

In this section, we examine the spatial pattern and size of O_3 and $PM_{2.5}$ concentration changes driven by the effects of BEs on atmospheric chemical system in the SMA. Conversely, it can provide useful information to understand how anthropogenic emissions spatially interact with BEs in the course of O_3 and PM formations in the SMA. For this analysis, the raw CMAQ data sets are used because the data fusion were not conducted for precursor species of O_3 and PM due to lack of data. Because the [A]-to-[A + B] ratios for O_3 and PM remain stable before and after the OBF in the model domain, CMAQ-raw data can be used to analyze the patterns of O_3 and PM changes associated with BEs in the SMA. Simulated monthly changes in daily maximum 8-h O_3 (hereafter, O_3) and mean 24-h $PM_{2.5}$ ($PM_{2.5}$) concentrations are illustrated in Fig. 5.

The predicted monthly average daily O_3 concentrations for the [A] scenario in the SMA were 46.54 ppb, 27.46 ppb in Seoul, 50.61 ppb in Incheon, and 46.37 ppb in Gyeonggi. Due to the effects of BEs, O_3 increased by 16.97% (7.90 ppb) across the SMA (Fig. 5a,b). Seoul, 24.90% (6.84 ppb), showed the largest rate of O_3 increase, followed by Incheon, 17.51% (8.86 ppb), and Gyeonggi, 16.71% (7.75 ppb). These widespread O_3 patterns of increase are due to an accelerated NO_2–NO–O_3 cycling system connected to the VOC oxidation cycle in the study domain. In the atmospheric VOC oxidation cycle, increases in NMVOC (Fig. S4, a1–a3) dominate because the additional BEs consume significant hydroxyl radicals ($OH^{\cdot}$) (Fig. S4, c1–c3) and produce additional oxidants (e.g., organic peroxy ($RO_2^{\cdot}$) and hydroperoxy ($HO_2^{\cdot}$) radicals) and a number of byproducts, such as secondary VOCs (SVOC, e.g., formaldehyde (HCHO) and methyl vinyl ketone

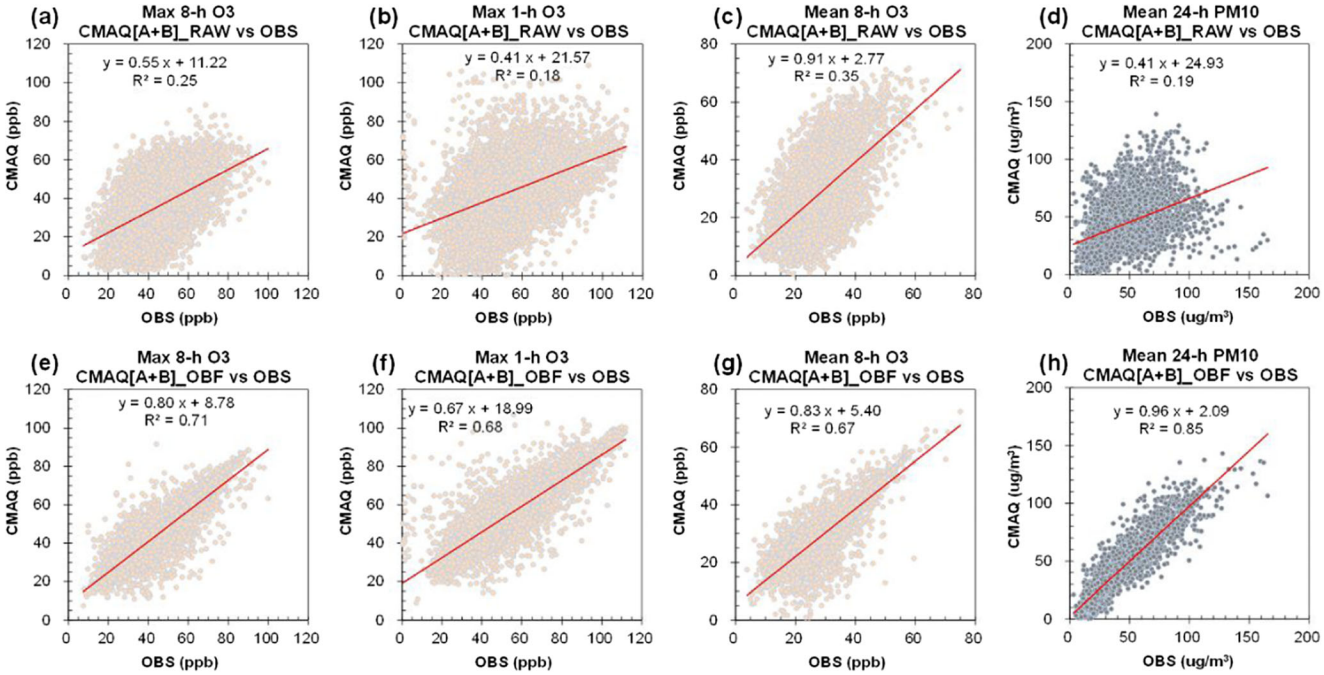

Fig. 4 Linear regression between observation (OBS) and predicted (CMAQ) daily averaged O_3 and PM10 concentrations for June 2008. The predictions are based on raw (**a**, **b**, **c**, and **d**) and observation data fused (**e**, **f**, **g**, and **h**) CMAQ results averaged at all monitoring stations

(MVK)) and numerous condensable products. Enriched peroxy radicals provide increased amounts of NO_2 to the NO_2–NO–O_3 cycling system in the domain by catalyzing the NO → NO_2 conversion and reproducing $OH^{\cdot}$. Then, very rapid photodissociation of NO_2 produces oxygen atoms and leads to daytime O_3 production in the domain. However, at nighttime, O_3 titration by NO from both biogenic and anthropogenic sources causes NO_2 regeneration which in turn leads to NO_3 radical formation and subsequent daytime formation of HNO_3. The daytime HNO_3 production is known to be a major sink of NO_x. In most SMA in early summer, however, HNO_3 formation was most likely not important for the destruction of NO_x due to widespread effects of biogenically emitted VOC concentrations on photochemical environment. Rather than HNO_3 formation reaction, peroxyacetylnitrate (PAN) production increased in importance as the radical environment is shifted in favor of peroxy radicals due to large increase in VOC levels relative to NO_x in most SMA (e.g., Fig. S4, e1–e3). Namely, abundant peroxyacetyl radicals ($CH_3C(O)OO^{\cdot}$) due to additional oxidations of SVOC significantly increase the concentration of peroxyacetylnitrate (PAN) in the domain (Fig. S4, b1–b3) via reactions with NO_2 (Seinfeld and Pandis 1998). Consequently, the domain experienced a significant increase in the O_3 (Fig. 5a,b) and overall decrease in the NO_x concentration except in some northern boundary areas where they showed some increases (0.1–6%) in the NO_x concentration (Fig. S4, d1–d3) due to the influence of locally emitted biogenic NO (Fig. 3e).

The predicted monthly average $PM_{2.5}$ concentrations with [A] scenario were 19.2 μg m^{-3} in the SMA, 44.94 μg m^{-3} in Seoul, 18.29 μg m^{-3} in Incheon, and 18.90 μg m^{-3} in Gyeonggi. Due to the addition of BEs, $PM_{2.5}$ concentration increased by 1.0% (0.2 μg m^{-3}) on average across the SMA, with a maximum increasing concentration of 0.7 μg m^{-3}

Table 3 Summary of the model performance evaluation for the O_3 and $PM_{2.5}$ air quality metrics after observation data fusion (OBF). "Obs" indicates observed concentrations

O_3	Mean (ppb)			MB (ppb)		NMB (%)		NME (%)		R^2	
(147 sites)	Obs	[A + B]	[A]	[A + B]	[A]	[A + B]	[A]	[A + B]	[A]	[A + B]	[A]
Max 8-h	46.00	45.73	37.49	− 0.27	− 8.50	− 0.58	− 18.49	11.76	23.16	0.71	0.59
Max 1-h	53.40	54.04	44.15	0.63	− 9.25	1.19	− 17.32	16.24	24.90	0.68	0.52
Mean 8-h	29.12	29.56	24.35	0.43	− 4.78	1.92	− 16.05	13.33	22.76	0.67	0.59
PM_{10}	Mean (μg m^{-3})			MB (μg m^{-3})		MFB (%)		MFE (%)		R^2	
(147 sites)	Obs.	[A + B]	[A]	[A + B]	[A]	[A + B]	[A]	[A + B]	[A]	[A + B]	[A]
Mean 24-h	45.91	45.27	45.08	− 0.64	− 0.83	− 3.11	− 3.61	20.87	21.12	0.85	0.84

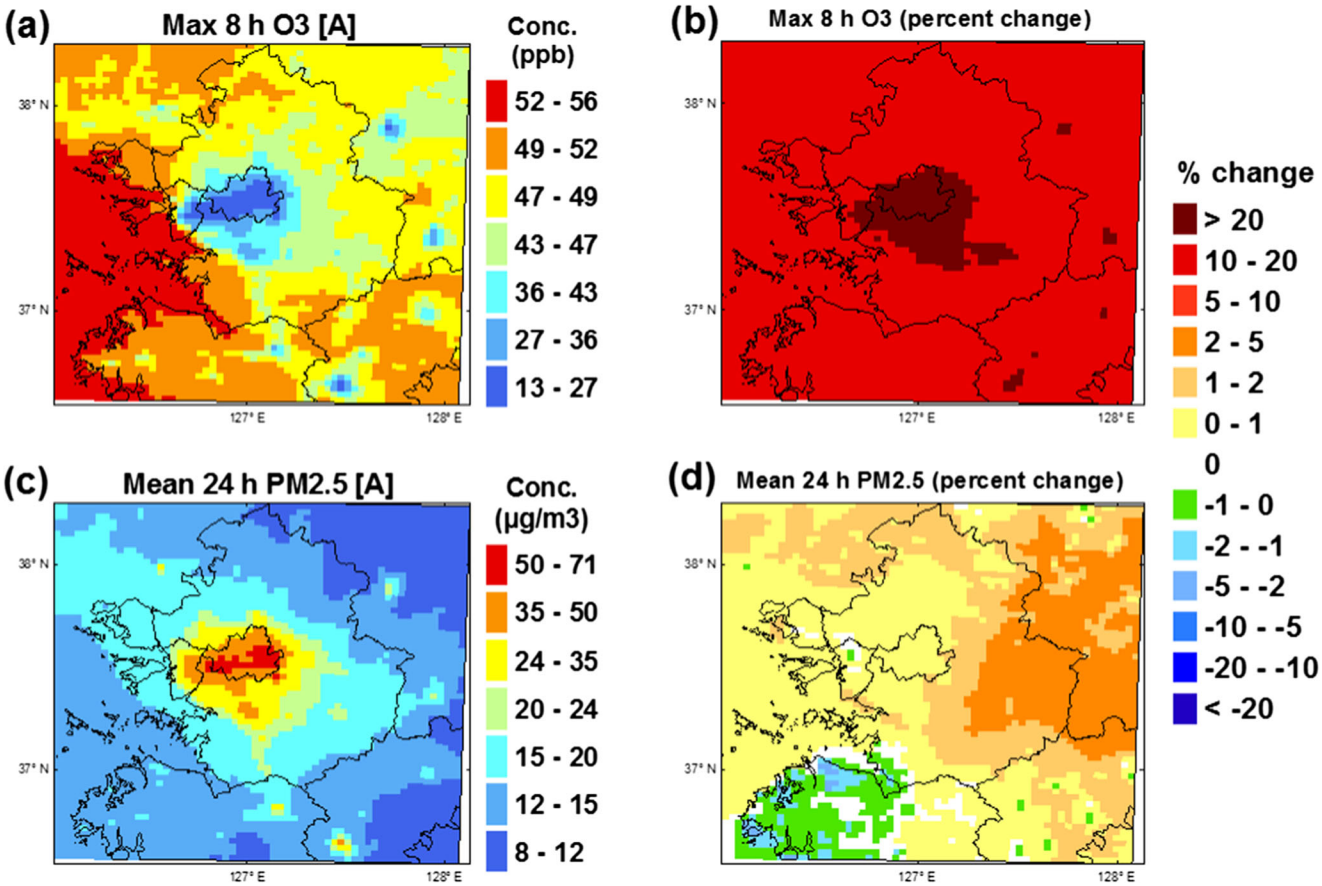

Fig. 5 Monthly averaged concentrations of O_3 and $PM_{2.5}$ for the anthropogenic-only case and percent changes in these concentrations due to the added biogenic emission (BE) effects: (**a**) maximum 8-h O_3, (**b**) mean 24-h $PM_{2.5}$, (**c**) changes in maximum 8-h O_3, and (**d**) changes in mean 24-h $PM_{2.5}$

(1.06%) in eastern Gyeonggi (Fig. 5c,d), which showed higher increase in NMVOC emissions (Fig. 3a–c). Conversely, some southwestern areas, e.g., in Gyeonggi and Chungnam, showed a slight decrease in $PM_{2.5}$, 0.5% (0.08 μg m^{-3}) on average, with a maximum of 0.4 μg m^{-3} (Fig. 5c,d). Possible causes of these trends will be presented later in this section. In the SMA, Gyeonggi showed the largest increasing rate, 1.16% (0.22 μg m^{-3}), followed by Seoul, 0.62% (0.28 μg m^{-3}), and Incheon, 0.48% (0.09 μg m^{-3}). Biogenic secondary organic aerosols (BSOAs) were the major contributors to the domain-wide $PM_{2.5}$ increase, except for some southwestern areas. Supplemented NMVOC budgets by BEs, e.g., monoterpene and some aromatic compounds, enhanced SOA formation via reactions with atmospheric oxidants (Atkinson 2000; Odum et al. 1997; Platt et al. 1990; Winer et al. 1984). While this resulted in an increase in SOAs (Fig. 6a,b), the concentrations of oxidants somewhat decreased (Fig. S4, c1–c3 and Fig. S4, f1–f3).

The predicted decrease in secondary inorganic aerosols (SIOAs) was accompanied by the increase in SOAs across the domain (Fig. 6). It should be noted that SIOAs are attributed only to anthropogenic sources (SIOAs = sulfate aerosols (ASO_4) + ammonium aerosols (ANH_4) + nitrate aerosols (ANO_3)), while SOAs include both anthropogenic and biogenic sources (i.e., SOAs = ASOAs + BSOAs). Across the domain, the increase and decrease in the SOA and SIOA concentration amounted to 0.42 and 0.26 μg m^{-3}, respectively. Consequently, the net increase in the $PM_{2.5}$ concentration was 0.16 μg m^{-3}. The changes in $PM_{2.5}$ in the SMA, including Seoul, Incheon, and Gyeonggi, can be explained in a similar way (Table 4). The contribution of changes in ASOAs to the total SOA mass change across the domain was less than 5%, suggesting that the increase in BSOAs was a major cause of the net increase in $PM_{2.5}$ levels. In contrast, the slight decrease in predicted $PM_{2.5}$ in some Gyeonggi and southwestern areas was associated with a relatively large decrease in SIOAs (see Table 4). Over the areas where $PM_{2.5}$ decreased, the average SOA increase was 0.26 μg m^{-3} and SIOA decrease was 0.38 μg m^{-3}, and the net decrease in $PM_{2.5}$ was 0.12 μg m^{-3}. Meanwhile, it should be noted that using more recent version of models equipped with more advanced aerosol mechanisms may better simulate increases in SOAs due to emission changes (e.g., Carlton et al. 2010).

The overall decreasing trends in SIOAs (Fig. 6c,d) were mainly affected by the parallel decreasing trends in important oxidants, such as $OH^{\cdot}$ (Fig. S4, c1–c3) and NO_3 (Fig. S4, f1–

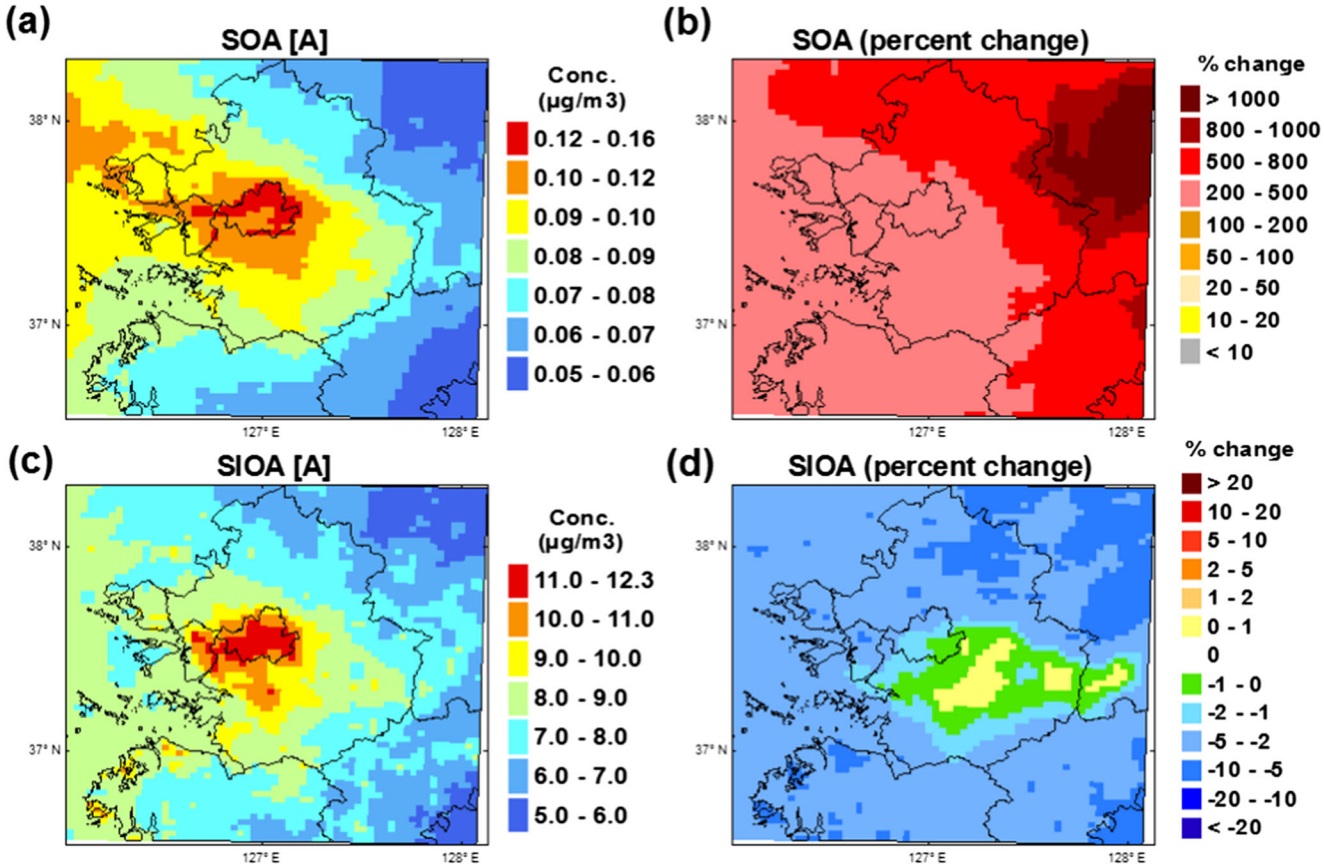

Fig. 6 Monthly averaged concentrations of secondary PM components for the anthropogenic-only case and percent changes in these concentrations due to the added effects of BEs: (**a**) and (**b**) show SOA and SIOA concentrations, respectively. (**c**) and (**d**) show the changes in SOA and SIOA concentrations, respectively

f3) in the SMA, except for Seoul and some Incheon and Gyeonggi areas. Due to the addition of BEs in the O_3 and SOA formation cycles, the average OH and NO_3 levels decreased on average 65% and 47% over the land area and 58% and 42% over the SMA region, respectively. These decreases in OH and NO_3 slow down the overall production of the major precursors of SIOA such as HNO_3 and sulfuric acid (H_2SO_4) in the domain. Unlike other areas, there were increases in $OH^{\cdot}$ and NO_3 in Seoul and some Incheon and Gyeonggi areas where high concentrations of anthropogenic NO_x are emitted (Fig. 2c). The OH increase in these areas can be explained by the enhanced $OH^{\cdot}$ recycling (i.e., $HO_2^{\cdot} + NO \rightarrow OH^{\cdot} + NO_2$) in these areas due to the added biogenic NO emissions. This explanation is supported by strong positive correlations between OH and NO emission changes (Fig. S5, a) and significant contribution of westerly–northwesterly and easterly–northeasterly flows to mean OH concentration (Fig. S5, b) in the OH-increasing areas (see the figure insets in Fig. S5, a). Namely, the OH concentrations in those areas were nonlinearly or linearly increased by both added NO concentrations from inner biogenic sources and transportation from surrounding biogenic source areas. This indicates that biogenic NO emissions play a significant source of the OH increase in major anthropogenic NO_x source areas in the SMA. On the

Table 4 Changes in the monthly average of the daily mean 24-h $PM_{2.5}$ concentrations attributed to the net changes in the monthly average of secondary organic aerosol (SOA) and secondary inorganic aerosol (SIOA) concentrations in the SMA region and $PM_{2.5}$-decreasing areas (unit μg m^{-3})

Region	$PM_{2.5}$ (% change)	SOA (% change)	SIOA (% change)
SMA	0.20 (1.05)	0.43 (473.77)	− 0.23 (− 2.72)
Seoul	0.28 (0.62)	0.47 (375.00)	− 0.19 (− 1.75)
Incheon	0.09 (0.48)	0.37 (374.79)	− 0.28 (− 3.30)
Gyeonggi	0.22 (1.16)	0.44 (496.78)	− 0.22 (− 2.67)
PM-decreasing areas	− 0.12 (− 0.89)	0.26 (325.81)	− 0.38 (− 4.62)

other hand, although more active O_3 photolysis due to increasing O_3 levels also can facilitate the OH increase (Han et al. 2013; Atkinson 2000), significant correlation between the O_3 and the OH change was not observed in the selected OH-increasing areas (graphical result is not seen here). This reaffirms a major contribution of biogenic NO sources to the OH increase. With these surplus $OH^{\cdot}$ concentrations, the VOC oxidation and NO_2–NO–O_3 cycles can become more active, and NO_3 production can be somewhat enhanced in those areas. These explanations are supported by the increase in NO_3 levels, by 45% on average, exceeding those in high anthropogenic NO_x-emitting areas (i.e., OH-increasing areas) (Fig. S4, f1–f3). A slight increase in HNO_3 (average 1% and maximum 4%) in the southern part of Seoul and its vicinity (Fig. S4, g1–g3) areas is also partly associated with such $OH^{\cdot}$ increase.

Mortality impacts and interrelationship with pollution variables

We calculated excess all-cause mortality due to short-term exposure to O_3 and $PM_{2.5}$ concentrations attributable to BEs. We used the observation-fused CMAQ results for maximum 8-h O_3 and 24-h mean $PM_{2.5}$ concentrations and the corresponding HIF parameters from the most recent epidemiological studies over multiple East Asian cities (Table 1). Daily O_3- and $PM_{2.5}$-related all-cause mortalities were calculated at each model grid and geographically aggregated (Table 5).

We estimate 62 (95% confidence interval 49–76) all-cause premature mortalities in the SMA from short-term changes in O_3 concentrations associated with the influence of BEs during June 2008. This is comparable to annual mortality impacts (51 premature deaths) of O_3 in California in 2005 attributable to emissions from two major sectors in the United States, such as electric power generation and industry (Caiazzo et al. 2013). We also estimate (22 (95% CI 18–28)) all-cause premature deaths in Seoul in this study. This corresponds to approximately 65% of the avoidable annual all-cause deaths (34 (95% CI − 23 to 90)) for the 0–64-year age group in Seoul in 2005 when attaining the WHO guidelines of daily maximum 8-h O_3 (100 μg $m^{-3} \approx 50$ ppb) (Bae and Park 2009). Although these comparisons have some limitations, such as differences in HIF parameter, study period, and age group, these suggest how significantly large the impact of biogenic emissions on the O_3-related mortality estimations are.

In the previous section, we observed that O_3 and PM aerosol formations in the SMA share nonlinear functions of inorganic and organic precursor species from either or both anthropogenic and biogenic sources (Meng et al. 1997). As the risk-based air quality management focusing on reductions of the O_3- and $PM_{2.5}$-related population health impacts is being highlighted in the SMA (i.e., SMAQIP-II), anthropogenic sources of O_3 and $PM_{2.5}$ precursors are expected to be controlled as the priority targets (Hogrefe et al. 2011). In reality, it has been reported that over the past two decades, local and regional management of precursor emissions has contributed to reducing the occurrence of peak O_3 episodes across Europe (e.g., Borrego et al. (2016) and references therein). Therefore, potential air policies in the SMA need to carefully consider about how the O_3 and $PM_{2.5}$ concentrations and related health risks will respond to the changes in their anthropogenic precursor concentrations in the presence of BEs. Namely, exploring these connections could provide useful information for the right direction of reducing O_3- and $PM_{2.5}$-related health risks in the SMA. In this sense, we examined the changes in the simulated O_3 and $PM_{2.5}$ levels and associated mortality rates as a function of the simulated VOC/NO_x ratios (unit ppb C/ppb) in the SMA (Fig. 7). It should be noted that we did not examine this for the $PM_{2.5}$ case due to little impact of BEs on $PM_{2.5}$ and the mortalities across the SMA.

As shown in Fig. 7, the predicted VOC/NO_x ratios across the SMA fall between 0.4 and 5.1 ppb C/ppb. The predicted O_3 concentrations range from about 26 ppb over the strong VOC-limited locations to 68 ppb over somewhat NO_x-limited locations in the SMA. Correspondingly, the estimated MR values range from about 0.1 to 0.7 in the SMA. Polynomial regression plots show that the predicted O_3 concentrations ([A + B] case) are strongly correlated with the predicted VOC/NO_x ratios ($r = 0.81$) (Fig. 7a) and the estimated MR are also significantly correlated with the VOC/NO_x ratios

Table 5 Spatially aggregated monthly all-cause mortalities for O_3 and $PM_{2.5}$ attributable to the effects of BEs (period June 2008). Monthly O_3 and $PM_{2.5}$ concentrations with the [A] case and resulted changes in O_3 and $PM_{2.5}$ concentrations (i.e., ΔC) due to the effects of BEs are also summarized

Region	Max 8-h O_3			Mean 24-h $PM_{2.5}$		
	Mortality (95% CI)	[A] (ppb)	ΔC (% change)	Mortality (95% CI)	[A] (μg m^{-3})	ΔC (% change)
SMA	62 (49–76)	49.22	8.43 ppb (17.48)	0.49 (− 0.08 to 1.04)	29.27	0.30 μg m^{-3} (1.13)
Seoul	22 (18–28)	34.06	8.52 ppb (25.66)	0.19 (− 0.03 to 0.4)	37.69	0.22 μg m^{-3} (0.60)
Incheon	7 (6–9)	51.28	9.23 ppb (18.15)	0.00 (− 0.00 to 0.01)	31.24	0.13 μg m^{-3} (0.43)
Gyeonggi	32 (26–40)	49.31	8.28 ppb (17.07)	0.29 (− 0.05 to 0.63)	28.72	0.33 μg m^{-3} (1.26)
Other areas	10 (8–12)	52.50	8.51 ppb (16.24)	0.08 (− 0.01 to 0.17)	25.92	0.28 μg m^{-3} (1.21)

($r = 0.51$) (Fig. 7b). In very VOC-sensitive locations (i.e., [L] zone) where the VOC/NO_x ratios range from 0.4 to 1.4, the O_3 concentrations and the MR were predicted to logarithmically increase. Whereas, in the [H] zone (VOC/NO_x = 2.2–5.1), the O_3 concentrations and MR were predicted to increase in the form of exponential function. Meanwhile, in the [M] zone (VOC/NO_x = 1.4–2.2), the O_3 concentrations were simulated to plateau, while MR continued to increase slightly. The O_3 concentrations at the locations in both [L] and [H] zones would apparently to be reduced effectively by lowering VOC/NO_x ratios by controlling anthropogenic VOC rather than NO_x emissions. Consequently, this would benefit to reduce population mortality risks in those zones. In contrast, in the mid-level VOC/NO_x ratio zone (i.e., [M] zone), it is not clear whether the effective means are VOC-only reductions or a combination of VOC and NO_x for reducing O_3. The trend lines in the [M] zone in Fig. 7a,b imply that VOC reduction would decrease the MR slightly but steadily although it may not effectively reduce O_3 concentrations. Thus, steady VOC reductions would be necessary in terms of the mortality risk reductions in this zone.

The linear log–log plots shown in the insets in the figures support our overall idea stated previously by allowing a concise statistical interpretation. For example, the linear relationships of log [O_3] and log [MR] to log [VOC/NO_x] indicate that a 10% (about 0.16) decrease in the VOC/NO_x ratios is associated with a 1.5% (about 0.9 ppb) decrease in the O_3 levels and a 4.3% (about 0.014) decrease in the MR on average across the SMA, respectively (mean VOC/NO_x = 1.6, mean O_3 = 57 ppb, and mean MR = 0.33). Meanwhile, VOC control may not have spatially uniform effect on the O_3 and MR changes because the scattering ranges of O_3 and MR as a function of VOC/NO_x in the SMA are large.

Limitations in this experiment

Although the CMAQ-based O_3 and PM air quality metrics (i.e., raw CMAQ output) generally capture the observed values across the SMA region, these exhibited underestimation errors. Similarly, previous CMAQ model evaluations in the US revealed that all recent versions of the CMAQ models (i.e., CMAQ versions 4.6, 4.7, 5.02, and 5.1) tend to underestimate $PM_{2.5}$ concentrations in air quality station (AQS) sites at summer (Appel et al. 2017; Carlton et al. 2010). In contrast to $PM_{2.5}$, O_3 concentrations were consistently overestimated by all recent versions of the CMAQ models (i.e., CMAQ versions 4.6, 4.7, 5.02, and 5.1) in AQS sites in the US at summer (Appel et al. 2017; Chai et al. 2013; Foley et al. 2010). These imply that model biases noted in previous versions are inherited to the latest versions (Foley et al. 2010). Inadequate representation of atmospheric process in the applied air quality model is responsible for this systematic bias (Appel et al. 2017; Carlton et al. 2010; Foley et al. 2010).

Recent versions of CMAQ models include aerosol formation pathways from isoprene, alkenes, and polycyclic aromatic hydrocarbons (PAHs) to SOA (Appel et al. 2017; Foley et al. 2015; Carlton et al. 2010), but the CMAQ aerosol module in our model framework does not. However, updating with new models (i.e., CMAQ versions from 4.6 to 4.7 and 5.02 to 5.1) only led to an increment of less than 1 μg m^{-3} in the predicted daily $PM_{2.5}$ concentrations during summer in the US. Thus, using a recent version of CMAQ model (e.g., CMAQ version 4.7 or 5.1) would not significantly improve the observed negative biases in the predicted PM concentrations across the SMA region although it could result in larger increments of SOA over some locations with abundant BVOC sources compared to the CMAQv4.6. Due to these effects, the overall size

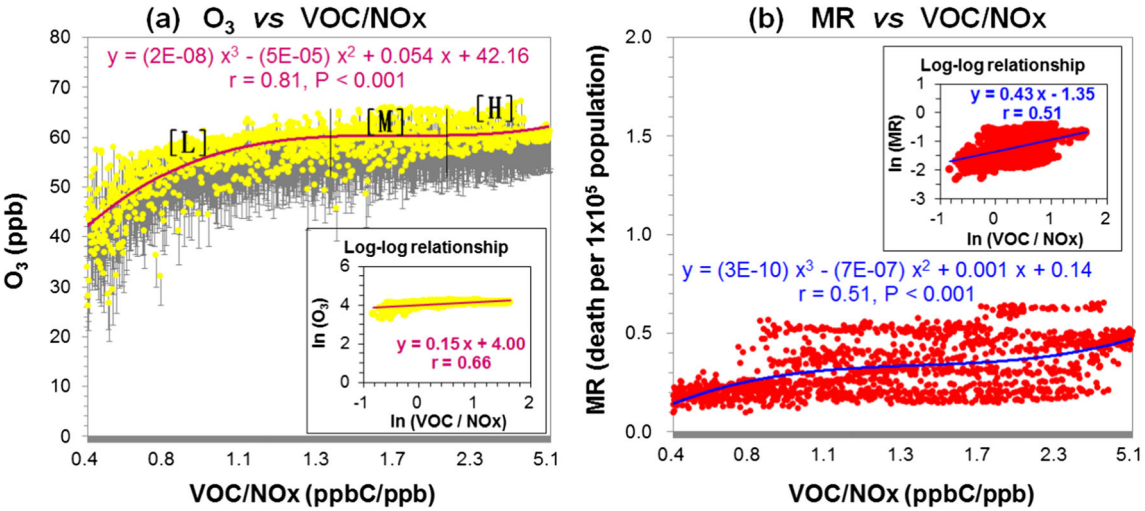

Fig. 7 Spatial distribution of monthly max 8-h O_3 ozone concentration (O_3) and mortality rate (MR) as a function of VOC/NO_x ratio across the SMA. MR is expressed in units of premature death per 100,000 people per month. Figure insets in (**a**) and (**b**) represent log–log relationships between the O_3 and VOC/NO_x and the MR and VOC/NO_x, respectively. Error bar in Fig. 7a indicates changes in O_3 concentrations due to the added effects of BE (i.e., ΔO_3). [L], [M], and [H] indicate the low, mid, and high VOC/NO_x ratio zones in the SMA, respectively

of $PM_{2.5}$ differences ($\Delta PM_{2.5}$) between the [A + B] and [A] scenarios are expected to be increased slightly in the SMA, thereby slightly increasing $PM_{2.5}$-related mortality estimates.

Unlike the case of $PM_{2.5}$, using a new version of CMAQ, particularly CMAQ version 5.1, could noticeably increase the predicted O_3 concentrations in the SMA. A recent model evaluation revealed that CMAQv5.1 updates to the clouds and photolysis calculations lead to generally higher O_3 mixing due to reduced cloudiness and attenuation of photolysis (i.e., reduced NO titration) compared to the previously released model, CMAQv5.02 (Appel et al. 2017). As a result, for the summer, CMAQv5.1 resulted in from 2.0 to 10.0 ppb increases in O_3 concentrations in the eastern US compared to CMAQv5.02. Large increases in daily O_3 concentrations were generally predicted in major urban areas. Thus, using a new version of CMAQ, e.g., CMAQ version 5.1, would lead to increase in the predicted O_3 concentrations in the SMA, especially over high NO_x-emitting urban city areas. As a result, the overall size of O_3 differences (ΔO_3) between the [A + B] and [A] scenarios are expected to be increased in the SMA, thereby causing increased O_3-related mortality estimates.

Collectively, using a new version of air quality model (i.e., CMAQv5.1) would reduce biases in the prediction of O_3 and $PM_{2.5}$ in certain levels in the SMA (e.g., Appel et al. 2017). However, this would have relatively small effect on the biases in O_3 and $PM_{2.5}$ predictions compared to the effect of bias-correction with observations (i.e., CMAQ-OBF) even if a new version of model can guarantee better predictions of O_3 and $PM_{2.5}$. Therefore, overall conclusions of our model study for BE-related O_3 and $PM_{2.5}$ air quality change and subsequent health impact assessment might not change significantly even under new model system setting.

Besides the model uncertainty, there are additional limitations to be noted for this study. First, city-specific values for the health impact function parameter (i.e., ER) were not applied during the O_3- and $PM_{2.5}$-related mortality estimations in the SMA due to the limited number of ERs for Korean metropolitan cities. Using the city-specific ER values could better represent city-specific air pollution-related health risk, thereby better supporting a risk-based air quality decision-making process. Another limitation is that the population input for HIA is based on the 2010 Korea population census data, but the real population during June 2008 may slightly differ from this. Finally, the length of the model experiment and the HIA in this study is not sufficiently long to establish a conclusive size of the impacts of BEs on O_3 and $PM_{2.5}$ change and related population mortality in the SMA.

Conclusions and recommendations

We investigated simulated changes in O_3 and $PM_{2.5}$ air quality concentrations due to the impact of BEs during an early summer period, and the subsequent effects on the population mortality in the SMA, where significant future control of anthropogenic precursor emissions is expected. For more improved mortality impact assessment, we utilized adjusted exposure fields for O_3 and $PM_{2.5}$ with an OBF method.

The results suggest that BE-involved atmospheric chemical processes (BEACP) that take place during early summer create a short-term O_3 air quality risk in the SMA, inducing increased population mortality. Unlike O_3, BEACP may not create significant burdens in terms of $PM_{2.5}$ air quality in the SMA, thereby inducing negligible effects on population mortality. The results also suggest that O_3 concentrations and related health risk in the SMA would be reduced through the steady efforts on VOC reductions from anthropogenic sources. For example, due to the effects of BEACP in June 2008, large mean increments of O_3, about 8.43 ppb, were responsible for approximately 62 all-cause premature mortalities in the SMA in June. Meanwhile, mean increment of $PM_{2.5}$ due to BEs was about 0.3 $\mu g\ m^{-3}$ and its health effect was negligible. A 10% decrease in the VOC/NO_x ratios through the VOC controls would lead to a 1.5% reduction in the O_3 levels and a 4.3% reduction in the MR on average across the SMA. The estimated size and trend of the mortality rates to the VOC/NO_x ratios may be useful to plan feasible controls for anthropogenic O_3 precursor emissions, thereby reducing health risks.

Follow-up studies may need to be conducted over additional periods, assuming other photochemical characteristics, and using more recent versions of models equipped with up-to-date algorithms so as to verify the representativeness of the results. These series of studies could provide strengthened scientific information to air and public health protection agencies pursuing risk-based air quality management. Despite several limitations, our work can be regarded as an important step for an improvement in scientific confidence in the connections between O_3, PM, and health risk in the presence of BEs and includes useful details for additional research to support the continual call for designing a risk-based air quality management in the SMA.

Acknowledgements This subject is supported by the Korean Ministry of Environment as "Climate Change Correspondence Program" (Project No. 2016001300001).

References

Appel KW, Napelenok SL, Foley KM, Pye HOT, Hogrefe C, Luecken DJ, Bash JO, Roselle SJ, Pleim JE, Foroutan H, Hutzell WT, Pouliot GA, Sarwar G, Fahey KM, Gantt B, Gilliam RC, Heath NK, Kang D, Mathur R, Schwede DB, Spero TL, Wong DC, Young JO (2017) Description and evaluation of the Community Multiscale Air Quality (CMAQ) modeling system version 5.1. Geosci Model Dev 10:1703–1732

Atkinson R (2000) Atmospheric chemistry of VOCs and NO_x. Atmos Environ 34:2063–2101

Atkinson R, Arey J (2003) Gas-phase tropospheric chemistry of biogenic volatile organic compounds: a review. Atmos Environ 37(SUPPL. 2):S197–S219

Bae HJ, Park J (2009) Health benefits of improving air quality in the rapidly aging Korean society. Sci Total Environ 407:5971–5977

Binkowski FS, Roselle SJ (2003) Models-3 Community Multiscale Air Quality (CMAQ) model aerosol component 1. Model description. J Geophys Res 108(D6):4183

Borrego C, Monteiro A, Martins H, Ferreira J, Fernandes AP, Rafael S, Miranda AI, Guevara M, Baldasano JM (2016) Air quality plan for ozone: an urgent need for North Portugal. Air Qual Atmos Health 9(5):447–460

Boylan JW, Russell AG (2006) PM and light extinction model performance metrics, goals, and criteria for three-dimensional air quality models. Atmos Environ 40(26):4946–4959

Byun DW, Schere KL (2006) Review of the governing equations, computational algorithms, and other components of the Models-3 Community Multiscale Air Quality (CMAQ) modeling system. Appl Mech Rev 59:51–77

Carlton AG, Bhave PV, Napelenok SL, Edney EO, Sarwar G, Pinder RW, Pouliot GA, Houyoux M (2010) Model representation of secondary organic aerosol in CMAQv4.7. Environ Sci Technol 44:8553–8560

Carter WPL (2000) Implementation of the SAPRC-99 chemical mechanism into the models-3 framework. United States Environmental Protection Agency, Washington D.C.

Caiazzo F, Ashok A, Waitz IA, Yim SH, Barrett SR (2013) Air pollution and early deaths in the United States. Part I: quantifying the impact of major sectors in 2005. Atmos Environ 79:198–208

Chai T, Kim HC, Lee P, Tong D, Pan L, Tang Y, Huang J, McQueen J, Tsidulko M, Stajner I (2013) Evaluation of the United States National Air Quality Forecast Capability experimental real-time predictions in 2010 using air quality system ozone and NO_2 measurements. Geosci Model Dev 6:1831–1850

Chatani S, Matsunaga SN, Nakatsuka S (2015) Estimate of biogenic VOC emissions in Japan and their effects on photochemical formation of ambient ozone and secondary organic aerosol. Atmos Environ 120:38–50

Chen R, Cai J, Meng X, Kim H, Honda Y, Guo YL, Samoli E, Yang X, Kan H (2014a) Ozone and daily mortality rate in 21 cities of East Asia: how does season modify the association? Am J Epidemiol 180:729–736

Chen G, Li J, Ying Q, Sherman S, Perkins N, Rajeshwari S, Mendola P (2014b) Evaluation of observation-fused regional air quality model results for population air pollution exposure estimation. Sci Total Environ 485–486:563–574

Dionisio KL, Baxter LK, Burke J, Özkaynak H (2016) The importance of the exposure metric in air pollution epidemiology studies: when does it matter, and why? Air Qual Atmos Health 9:495–502

Finlayson-Pitts BJ, Pitts JN Jr (2000) Chemistry of the upper and lower atmosphere. Academic Press, San Diego

Foley KM, Roselle SJ, Appel KW, Bhave PV, Pleim JE, Otte TL, Mathur R, Sarwar G, Young JO, Gilliam RC, Nolte CG, Kelly JT, Gilliland AB, Bash JO (2010) Incremental testing of the CMAQ modeling system version 4.7. Geosci Model Dev 3:205–226

Foley KM, Hogrefe C, Pouliot G, Possiel N, Roselle SJ, Simon H, Timin B (2015) Dynamic evaluation of CMAQ part I: separating the effects of changing emissions and changing meteorology on ozone levels between 2002 and 2005 in the eastern US. Atmos Environ 103:247–255

Grell GA, Dudhia J, Stauffer DR (1994) A description of the fifth-generation Penn State/NCAR mesoscale model (MM5), NCAR technical note, NCAR/TN-398+STR, 117

Guenther A, Karl T, Harley P, Wiedinmyer C, Palmer PI, Geron C (2006) Estimates of global terrestrial isoprene emissions using MEGAN (Model of Emissions of Gases and Aerosols from Nature). Atmos Chem Phys 6:3181–3210

Han KM, Park RS, Kim HK, Woo JH, Kim J, Song CH (2013) Uncertainty in biogenic isoprene emissions and its impacts on tropospheric chemistry in East Asia. Sci Total Environ 463-464:754–771

Hogrefe C, Isukapalli SS, Tang X, Georgopoulos PG, He S, Zalewsky EE, Hao W, Ku JY, Key T, Sistla G (2011) Impact of biogenic emission uncertainties on the simulated response of ozone and fine particulate matter to anthropogenic emission reductions. J Air Waste Manage Assoc 61:92–108

Huang R, Zhai X, Ivey CE, Friberg MD, Hu X, Liu Y, Di Q, Schwartz J, Mulholland JA, Russell AG (2017) Air pollutant exposure field modeling using air quality model-data fusion methods and comparison with satellite AOD-derived fields: application over North Carolina, USA. Air Qual Atmos Health 11:11–22

Hubbell BJ (2012) Understanding urban exposure environments: new research directions for informing implementation of US air quality standards. Air Qual Atmos Health 5(2):259–267

Kan H, London SJ, Chen G, Zhang Y, Song G, Zhao N, Jiang L, Chen B (2007) Differentiating the effects of fine and coarse particles on daily mortality in Shanghai, China. Environ Int 33(3):376–384

Kim H-K, Woo J-H, Park RS, Song CH, Kim JH, Ban SJ, Park JH (2014) Impacts of different plant functional types on ambient ozone predictions in the Seoul Metropolitan Areas (SMAs), Korea. Atmos Chem Phys 14(14):7461–7484

Kim SY, Jiang X, Lee M, Turnipseed A, Guenther A, Kim JC, Lee SJ, Kim S (2013) Impact of biogenic volatile organic compounds on ozone production at the Taehwa Research Forest near Seoul, South Korea. Atmos Environ 70:447–453

Lee H, Honda Y, Hashizume M, Guo YL, Wu CF, Kan H, Jung K, Lim YH, Yi S, Kim H (2015) Short-term exposure to fine and coarse particles and mortality: a multicity time-series study in East Asia. Environ Pollut 207:43–51

Ministry of Environment (MoE) (2015) Ecorea: environmental review. Ministry of Environment, Sejong, p 2013

Meng Z, Dabdub D, Seinfeld JH (1997) Chemical coupling between atmospheric ozone and particulate matter. Science 277:116–119

Nenes A, Pandis S, Pilinis C (1998) ISORROPIA: a new thermodynamic equilibrium model for multiphase multicomponent inorganic aerosols. Aquat Geochem 4(1):123–152

Odum JR, Jungkamp TPW, Griffin RJ, Flagan RC, Seinfeld JH (1997) The atmospheric aerosol-forming potential of whole gasoline vapor. Science 276(5309):96–99

Park RS, Cho Y-K, Choi B-J, Song CH (2011) Implications of sea surface temperature deviations in the prediction of wind and precipitable water over the Yellow Sea. J Geophys Res 116(D17):D17106

Pebesma E, Graeler B (2018) Package "gstat," CRAN reference manual. Available: https://cran.r-project.org/web/packages/gstat/gstat.pdf. Accessed 17 April 2018

Platt U, LeBras G, Poulet G, Burrows JP, Moortgat G (1990) Peroxy radicals from night-time reaction of NO_3 with organic compounds. Nature 348(6297):147–149

R Core Team (2018) R: a language and environment for statistical computing. R Foundation for Statistical Computing, Vienna URL https://www.R-project.org/

Russell AG, Dennis R (2000) NARSTO critical review of photochemical models and modeling. Atmos Environ 34(12–14):2283–2324

Schell B, Ackermann IJ, Hass H, Binkowski FS, Ebel A (2001) Modeling the formation of secondary organic aerosol within a comprehensive air quality model system. J Geophys Res 106(D22):28275–28293

Seinfeld JH, Pandis SN (1998) Atmospheric chemistry and physics: from air pollution to climate change, New York, U.S

Streets DG, Bond TC, Carmichael GR, Fernandes SD, Fu Q, He D, Klimont Z, Nelson SM, Tsai NY, Wang MQ, Woo JH, Yarber KF (2003) An inventory of gaseous and primary aerosol emissions in Asia in the year 2000. J Geophys Res 108(D21):8809

US EPA (Environmental Protection Agency) (2012) BenMAP user's manual appendices. Available: http://www.epa.gov/oaqps001/benmap/models/BenMAPAppendicesOct2012.pdf. Accessed 17 April 2014

Wesson K, Fann N, Morris M, Fox T, Hubbell B (2010) A multi-pollutant, risk-based approach to air quality management: case study for Detroit. Atmos Pollut Res 1:296–304

WHO (1994) International classification of diseases, Tenth revision edn. World Health Organization, Geneva

WHO (2013) Review of evidence on health aspects of air pollution. REVIHAAP project technical report. WHO Regional Office for Europe, Bonn

Winer AM, Atkinson R, Pitts JN (1984) Gaseous nitrate radical: possible nighttime atmospheric sink for biogenic organic compounds. Science 224:156–159

Woo J-H, Choi K-C, Kim H-K, Baek BH, Jang M, Eum J-H, Song CH, Ma Y-I, Sunwoo Y, Chang L-S, Yoo SH (2012) Development of an anthropogenic emissions processing system for Asia using SMOKE. Atmos Environ 58:5–13

Zhang Q, Streets DG, Carmichael GR, He KB, Huo H, Kannari A, Klimont Z, Park IS, Reddy S, Fu JS, Chen D, Duan L, Lei Y, Wang LT, Yao ZL (2009) Asian emissions in 2006 for the NASA INTEX-B mission. Atmos Chem Phys 9(14):5131–5153